TUNING METHODS FOR HIMAC MULTIPLE-ENERGY OPERATION

Ken KATAGIRI, Takuji FURUKAWA, Kota MIZUSHIMA, Shinji SATO, Yoshiyuki IWATA, Toshiyuki SHIRAI, and Koji NODA,
Medical Physics Research Group, National Institute of Radiological Sciences, Chiba, Japan

Abstract

Beam stability of the multiple-energy operation at HIMAC synchrotron was improved for the fast raster-scanning irradiation. In order to improve the transverse stability, the working point of the betatron tune was investigated during the acceleration section. The signals were collected from the beam position monitor using a fast data-acquisition unit. The temporal evolution of the horizontal and vertical betatron tune was evaluated by using the short time Fourier transforms. Analysed results showed that the working point of the betatron tune in the acceleration section passed thorough the 3rd- and 4th -order coupling resonance line. In order to keep the working point within the desirable operating region, the current patterns of the power supplies for the quadrupole magnets were corrected by using the variation of the betatron tune. The experimental results showed that the working point could be successfully stabilized, and the undesirable beam losses could be reduced during the acceleration section.

INTRODUCTION

A new control method was applied to HIMAC (Heavy-Ion Medical Accelerator in Chiba) synchrotron [1] for the fast raster-scanning irradiation [2]. This new operation method uses variable-energy patterns to change the beam energy during one operation cycle, and it can reduce the treatment time because the irradiation can be finished during the operation cycle without any additional injection of beams to the ring.

For the multiple-energy operation method, the operation patterns for all elements in the main ring were newly designed. Although it was determined that the current patterns of the dipole/quadrupole magnet were consistent with the frequency pattern of the acceleration RF cavity [3], there are tracking errors especially during the beginning region of the acceleration. This tracking errors lead to the variation of the betatron oscillation. If the variation of the betatron tune is large enough to passed thorough the resonance line, beam losses as well as emittance growth will occur.

In order to reduce the treatment time, it is necessary to finish the irradiation during one cycle operation without any additional injection. Therefore, the beam losses are not preferable to efficiently use the beams in the ring. For this reason, we optimized the current patterns of quadrupole magnet to suppress the variation of the betatron tune. The temporal evolutions of horizontal/vertical betatron tune were evaluated from the signal of BPM (Beam Position Monitor). By using the analyzed data, current patterns of QF (quadrupole focusing) and QD (quadrupole defocusing) magnet were corrected. In this paper, we present the effect of this tuning method on the variation of the betatron tune and the beam losses.

TUNING METHODS

Figure 1 shows the schematic diagram of the tune measurements. The subtraction signals of the BPM were collected for the horizontal/vertical tune measurement by using data acquisition unit (YOKOGAWA, SL1000). The sampling rate of the data acquisition was set to be 5 MS/s, which provides adequate frequency span for the tune observation from the spectrum of $\delta Q \cdot f_{rev}$ (δQ : fraction part of the betatron tune, f_{rev}: revolution frequency). Table 1 shows the experimental parameters for the tune measurements. The synchrotron was operated without the extended flattop mode [1], and its operation cycle was 3.3 seconds.

The temporal evolutions of the spectrum distribution were evaluated by the Short-Time Fourier Transform (STFT) with the Blackman–Harris window. The frequency resolution was set to be $\Delta f \approx 150$ Hz by the window length of $\Delta T = 6.55 \times 10^{-3}$ s. We can observe the

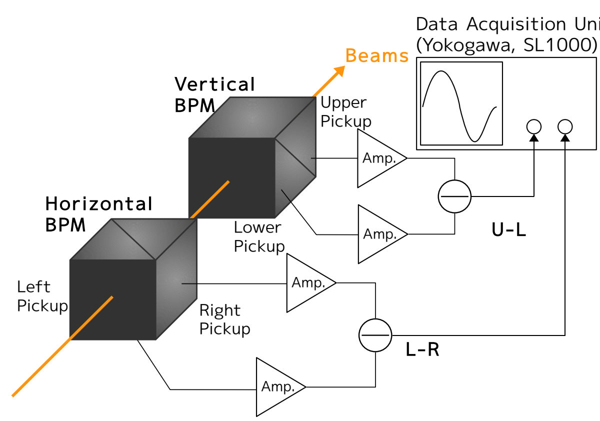

Fig. 1: Schematic diagram of the tune measurements.

Table 1: Experimental parameters of the HIMAC synchrotron.

Beam species		$^{12}C^{6+}$ ion
Beam energy (flat-base / 1st flat-top)	[MeV/u]	6 / 430
Revolution frequency (flat-base / 1st flat-top)	[MHz]	0.21 / 1.69
QF and QD current (flat-base / 1st flat-top)	[A]	QF: 82 / 780 QD: 81 / 776
Betatron tune (Qx, Qy)		(3.68, 3.13)
Number of ions per cycle		~ 10^{10}
Circumference	[m]	129.6

tune variation of the order of $\Delta Q \sim 10^{-4}$ by this configuration. The overlap of the STFT window is set to be 90%.

The peak tracking for the spectrum of $\delta Q \cdot f_{rev}$ was performed for every window to obtain the temporal evolution of the betatron tune. The relation between the horizontal-tune variation $\Delta Qx(t)$ ($=Qx(t)-Qx_{preset}(t)$, $Qx_{preset}(t)$: preset value of the betatron tune) and the correction current $\Delta I_{\mathrm{QF\ and\ QD}}(t)$ is given as follows:

$$\Delta Qx(t) = \frac{1}{4\pi}\sum_{i:\mathrm{QF}}\frac{\beta_i K_{\mathrm{QF},i}\Delta I_{\mathrm{QF},i}(t)\Delta l_{\mathrm{QF},i}}{I_{\mathrm{QF},i}(t)} + \frac{1}{4\pi}\sum_{i:\mathrm{QD}}\frac{\beta_i K_{\mathrm{QD},i}\Delta I_{\mathrm{QD},i}(t)\Delta l_{\mathrm{QD},i}}{I_{\mathrm{QD},i}(t)} \quad (1)$$

Here, I_{QF}(t) and I_{QD}(t) are the preset current pattern, β_i is the beta function, K_{QF} and K_{QD} are the K-value for each magnet, and Δl_{QF} and Δl_{QD} are the effective length for each magnet. Assuming that the variation of the horizontal tune is mainly produced by the QF magnets, we neglected the second term of the right side of Eq. (1) to simplify the calculation. Furthermore, since the K_{QF}, $\Delta I_{\mathrm{QF}}(t)$, Δl_{QF} and $I_{\mathrm{QF}}(t)$ are same for all the QF magnets in HIMAC synchrotron, Eq. (1) could be rewritten as follows:

$$\Delta I_{\mathrm{QF}}(t) = \frac{4\pi}{\left(\sum_{i:\mathrm{QF}}\beta_i\right)K_{\mathrm{QF}}\Delta l_{\mathrm{QF}}} I_{\mathrm{QF}}(t)\Delta Q_{\mathrm{QF}}(t) \quad (2)$$

The correction current for QD could also be derived from the same way as above.

RESULTS AND DISCUSSION

Figure 2 shows an analyzed result of the spectrum distribution for the horizontal oscillation. The tracking

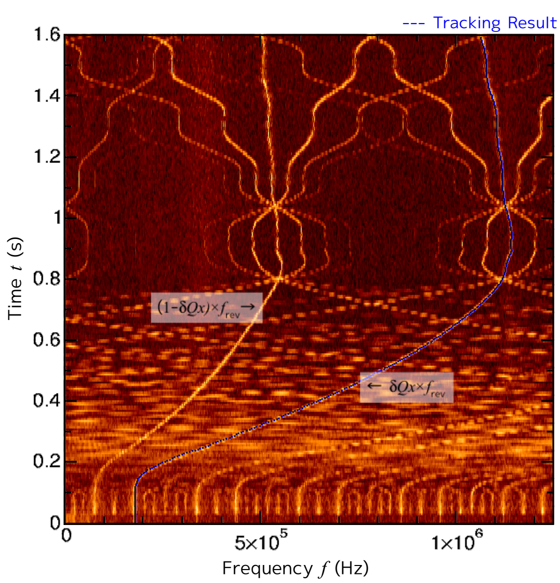

Fig. 2: Temporal evolution of the spectrum distribution for the horizontal oscillation.

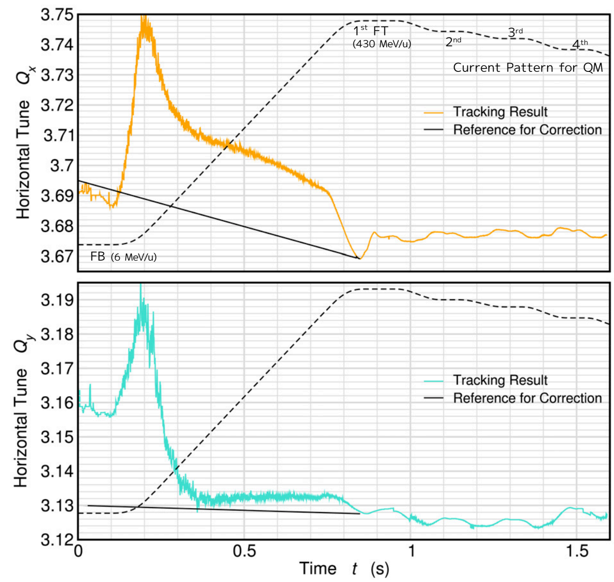

Fig. 3: Temporal evolution of the Qx and the Qy: Tracking result of the Fig. 2.

result is also plotted for comparison. We could clearly observe the spectrum caused by the betatron coherent oscillation, at $(1-\delta Qx) \cdot f_{rev}$ as well as $\delta Qx \cdot f_{rev}$. Although the betatron sidebands were present, we could obtain correct result of the peak tracking without large deviation.

Figure 3 shows a temporal evolution of horizontal/vertical tune. The current pattern of the QM magnet for variable energy operation is also plotted as a reference. Although the Qx and Qy deviate in the flattop section after $t \approx 0.9$ s, they were stabilized when each flattop is extended for the beam extractions [1]. At $t \approx 0.2$ s, when the acceleration begins, both Qx and Qy deviate extremely from ideal preset values, which are plotted as a black-solid line.

The time profiles of the betatron tune shown in Fig. 3 were used to evaluate the correction-current patterns for the QF and QD magnet. To cut off unnecessary noise for the power supply, the time profiles of the betatron tune

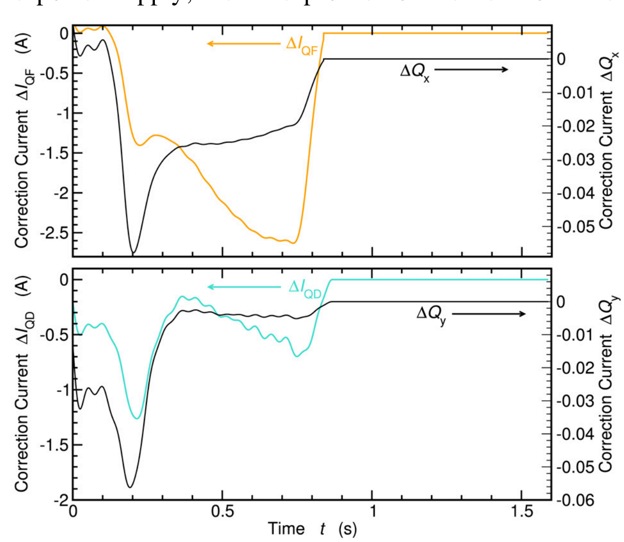

Fig. 4: Correction current for QF and QD magnet.

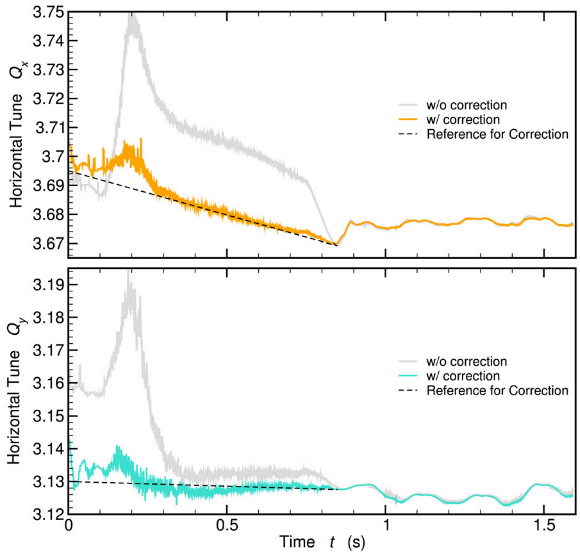

Fig. 5: Correction results of the time profile of the horizontal/vertical tune.

were filtered using 20-Hz low-pass filter. The tune deviation from the preset values were used as the tune variations of $\Delta Qx(t)$ and $\Delta Qy(t)$. The correction-current patterns evaluated from Eq. (2) are shown in Fig. 4. Although the absolute value of the $\Delta Qx(t)$ monotonically decreases after $t \approx 0.2$ s, the absolute value of the correction current ΔI_{QF} increases due to the growth of the current pattern $I_{QF}(t)$.

Figure 5 shows temporal evolutions of the horizontal/vertical tune after the correction. The results without correction were plotted as references. The time profiles of the corrected tunes could be controlled well along with the reference patterns without large deviation. We could also see that the large hump around $t \approx 0.2$ s was suppressed well for both Qx and Qy profiles.

In order to check the working point, the temporal evolutions of the horizontal and vertical tune were plotted in the tune diagram using all data during $t = 0 – 1.6$ s, as shown in Fig. 6. The blue symbols show the working points without correction, and the red symbols show that

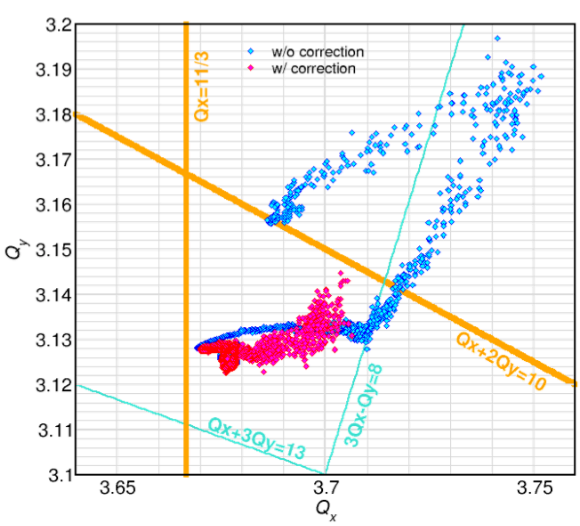

Fig. 6: Tune diagram for the tracking results.

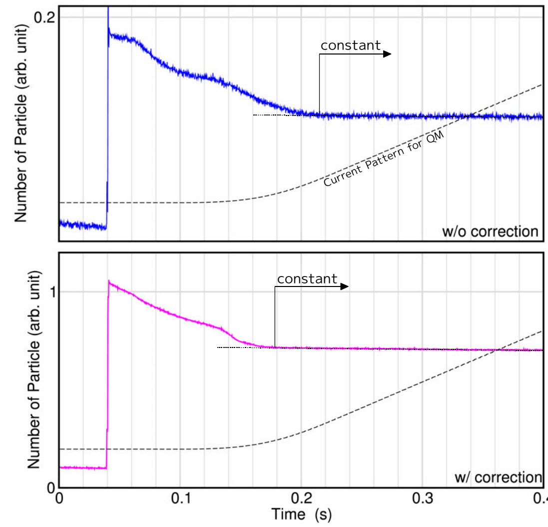

Fig. 7: Temporal evolutions of the number of the particle in the ring for the w/ and the w/o tune correction.

with correction. When the tune correction was not applied, the 3rd order resonance line of Qx+2Qy=10 and the 4th order resonance line of 3Qx–Qy=8 were passed through two times during the acceleration. We could see that, owing to the tune correction, the variation of the working points were stabilized in the region encircled by two lines of the 3rd order resonance and two lines of the 4th order resonance.

Figure 7 shows the temporal evolution of the number of particle in the ring for the w/o correction and the w/ correction. The number of the particle could not be compared because the initial number of the injected particles differs from each other. However, we could see that the beam losses, which occur at $t \approx 0.2$ s, could be suppressed by the tune correction.

CONCLUSION

Using the short time Fourier transforms, the temporal evolution of the horizontal and vertical betatron tune was evaluated from the BPM signals. The correction-current patterns for the QF/QD magnets were simply evaluated from the deviation of the tune profiles. Owing to the tune correction, the working points during the acceleration section were stabilized without passing through the 3rd and 4th resonance lines. In order to see clearly the effect of the tune correction on the beam stability, we are going to measure the transverse emittance by using a non-destructive beam-profile monitor [4].

REFERENCES

[1] Y. Iwata et al., Nucl. Instr. and Meth. A 624 (2010) 33.
[2] T. Furukawa, et al., Med. Phys. 37 (2010) 5672.
[3] T. Kadowaki, et al., Nucl. Instr. and Meth. A, in press.
[4] T. Honma, et al., Nucl. Instr. and Meth. A 490 (2002) 435.